Received: 27 July 2020 | Revised: 18 January 2021 | Accepted: 12 February 2021

IET Control Theory & Applications

DOI: 10.1049/cth2.12115

The Institution of Engineering and Technology WILEY

ORIGINAL RESEARCH PAPER

On the switching control of the DC–DC zeta converter operating in continuous conduction mode

Hafez Sarkawi[1,2] | **Yoshito Ohta**[1] | **Paolo Rapisarda**[3]

[1] Graduate School of Informatics, Kyoto University, Kyoto, Japan

[2] Fakulti Teknologi Kejuruteraan Elektrik dan Elektronik, Universiti Teknikal Malaysia Melaka, Melaka, Malaysia

[3] School of Electronics and Computer Science, University of Southampton, Southampton, UK

Correspondence
Hafez Sarkawi, Graduate School of Informatics, Kyoto University, Kyoto 606–8501, Japan.
Email: hafez@utem.edu.my

Abstract

Here, a switching control mechanism for the stabilization of a DC–DC zeta converter operating in continuous conduction mode is proposed. The switching control algorithm is based on a control Lyapunov function and extends the method proposed for a two-dimensional boost converter model presented in the literature to a four-dimensional zeta converter model. The local asymptotical stability of the operating point is established using LaSalle's invariance principle for differential inclusions. By applying spatial regularization, a modified switching control algorithm reduces the switching frequency and keeps the state-trajectory around a neighbourhood of the operating point. The method works well even if the operation point changes significantly and it is valid for both step-up and step-down operations. Furthermore, by approximating the state-trajectory near the operating point, an explicit relation between the modified switching algorithm and the switching frequency is obtained, which allows to choose systematically the desired switching frequency for the converter to operate. The effectiveness of the proposed method is illustrated with simulation results.

1 | INTRODUCTION

In energy harvesting systems, DC–DC converters are part of the power management system. Because of the uncertain nature of the ambient energy, for example, low or high irradiance of sun and fluctuation of the wind speed, the voltage generated by the energy harvester, which is connected to the input of the DC–DC converter, can be higher or lower than the output voltage. For this reason, a fourth-order DC–DC converter is a good candidate to be deployed, since it has step-up and step-down capability. There are a few topologies available, and the zeta topology is selected for our research due to two reasons: (1) positive output voltage, and low output voltage ripple [3], (2) natural DC input-to-output voltage isolation [4].

To control a DC–DC converter, the conventional fixed-frequency, average-based system control methods are commonly deployed such as proportional integral (PI) [5–9], optimal [11–16], sliding mode [17, 18], fuzzy [19, 20], model predictive [21, 22], adaptive [23], and fuzzy neural [24], to name a few. The PI control produces fast output voltage regulation, however, it suffers from high control duty-ratio effort [9] that can lead to PWM circuitry problem [12]. The conventional optimal linear quadratic regulator (LQR) control produces optimal compensation with minimal control effort, but lack of robustness if the parameter is uncertain [14]. While LMI-LQR control is robust, its control duty-ratio signal has quite a large ripple [15], which may produce non-linear effect if the ripple exceeded 20% [10]. As for the sliding mode, fuzzy, model predictive, adaptive, and fuzzy neural, because they use the so-called small-signal average model, when the duty ratio largely deviates from the nominal one, the small-signal average model is not a good approximation. As a result, the controller design is no longer valid, which in turn jeopardizes the system performance. On the other hand, non-average-based system control, typically known as hybrid control, is a variable switching frequency type of control where the switching frequency is initially low and it becomes arbitrarily fast at operating point. The hybrid control is more robust than average-based system control [2], due to the former's ability to execute the switching mechanism online. Hybrid control has been implemented for the stabilization of the DC–DC converter [25–32]. In [25–28], the authors propose a switching algorithm by approximating the state-trajectory and restricting the state-trajectory within a limits specified by the guard conditions. Even though the output voltage regulation is achieved and demonstrated, no theoretical work is presented to prove the stability of the system. In [29–32], the authors propose a Lyapunov-based hybrid control to stabilize the DC–DC converters. The study [29] basically proposes the switching rule that assigns the mode decreasing the value of the Lyapunov function most. When the trajectory reaches the switching boundary, it evolves as a sliding mode solution, which means that the switching interval becomes infinitesimally small. In [30, 31], the authors use sampled-data control to avoid sliding mode solutions. Though switching frequency is controlled by the sampling period, it tends to be small because the method is based on sufficient conditions. Hence the trajectory is close to the sliding solution. Though our paper uses the same switching mechanism as in [32], the stability analysis is fundamentally different. A second-order boost converter model in [32] can be analysed by the standard Lyapunov approach by showing the decrease of the Lyapunov function along the trajectory. The derivative along the trajectory of the fourth-order zeta converter model becomes zero even if the point is not the operating point. Hence LaSalle's invariance principle proved for this class of differential inclusion should be established. The preliminary and much shorter versions of our work were presented in the conference proceedings [1, 2].

The remainder of the paper is organized as follows. In Section 2, we establish a switching control mechanism for a two-mode system. The two-mode system is instrumental to model the DC–DC zeta converter operating in continuous conduction mode (CCM). In Section 3, we analyse the stability of the switching system in Section 2, and apply it to the zeta converter. In Section 4, the switching control mechanism discussed in Section 2 is modified to limit the switching frequency of the zeta converter. In addition, by using linear-line approximation of the trajectory, we show how to decide the switching frequency. Simulation results to show the effectiveness of our proposed method are presented in Section 5. Lastly, in Section 6, we conclude our work and state the plan for future work.

Notation: $\mathbb{R}$ denote the set of real numbers. For $\rho \in \mathbb{R}$, $\mathbb{R}_{>\rho}$, $\mathbb{R}_{<\rho}$, $\mathbb{R}_{\geq\rho}$, and $\mathbb{R}_{\leq\rho}$ denote the set of real numbers larger, smaller, larger than or equal to, and smaller than or equal to ρ, respectively. The notation conv denotes the convex hull of a set. For a function: $\mathbb{R}^n \to \mathbb{R}$, α^{-1} denotes the inverse image of α. For a singleton $\{c\}$, $c \in \mathbb{R}$, we use the simplified notation, $\alpha^{-1}(\mathrm{c}) = \alpha^{-1}(\{\mathrm{c}\})$. A set-valued map F is denoted as $F : \mathbb{R}^n \rightrightarrows \mathbb{R}^m$ where for $x \in \mathbb{R}^n$, $F(x) \subset \mathbb{R}^m$.

2 | SWITCHING CONTROL OF TWO-MODE SYSTEM

Because transistors and diodes exhibit on–off behaviours, many converters can be modelled as multi-mode systems, where each mode is described as a linear state-space model. A two-mode system can be used to model the CCM of any DC–DC converters. In this section, we introduce a Lyapunov-function-based switching control strategy and motivate its stability analysis.

Two linear systems of the same state dimension are given by

$$\frac{dx}{dt} = A_1 x + B_1 u, \tag{1}$$

$$\frac{dx}{dt} = A_2 x + B_2 u, \tag{2}$$

where $x(t) \in \mathbb{R}^n$ is the state and $u(t) \in \mathbb{R}$ is the input. Fix $u_0 \in \mathbb{R}$ and $\lambda \in \mathbb{R}$. Assume that

$$\lambda A_1 + (1-\lambda) A_2$$

is invertible. Define

$$x^* = -(\lambda A_1 + (1-\lambda) A_2)^{-1} (\lambda B_1 + (1-\lambda) B_2) u_0. \tag{3}$$

Note that we do not assume the stability nor the non-singularity of the matrices A_1 and A_2. Let $\mathcal{S}_i$ $(i = 1, 2)$ denote the set of stationary points of the systems (1) and (2); namely

$$\mathcal{S}_1 = \{x : A_1 x + B_1 u_0 = 0\}, \mathcal{S}_2 = \{x : A_2 x + B_2 u_0 = 0\}. \tag{4}$$

If A_i is non-singular, $\mathcal{S}_i$ is a singleton; otherwise it may be empty or infinite. The following proposition is easy to derive, but useful in the subsequent discussions.

Proposition 1. *The point x^* is given by (3) if and only if it satisfies the following equation:*

$$\lambda (A_1 x^* + B_1 u_0) = -(1-\lambda)(A_2 x^* + B_2 u_0). \tag{5}$$

Furthermore, $A_i x^* + B_i u_0 \neq 0$ $(i = 1, 2)$ if and only if $\mathcal{S}_1 \cap \mathcal{S}_2 = \emptyset$.

Proof. Since

$$(\lambda A_1 + (1-\lambda) A_2) x^* = (\lambda B_1 + (1-\lambda) B_2) u_0,$$

the equivalence of (3) and (5) is immediate. If $x^\# \in \mathcal{S}_1 \cap \mathcal{S}_2$, then

$$\lambda \left(A_1 x^\# + B_1 u_0\right) = -(1-\lambda) \left(A_2 x^\# + B_2 u_0\right) = 0,$$

which implies $x^\# = x^*$ by the non-singularity of $\lambda A_1 + (1-\lambda) A_2$. Conversely, if $A_1 x^* + B_1 u_0 = 0$, then $A_2 x^* + B_2 u_0 = 0$ by (5). Thus, $x^* \in \mathcal{S}_1 \cap \mathcal{S}_2$. □

We are interested in a switching control law that drives the state of the switching system with the modes (1) and (2) to x^* under $u(t) \equiv u_0$. For this, define a candidate Lyapunov function

$$V(x) = (x - x^*)^T P (x - x^*), \tag{6}$$

where P is a positive definite matrix. Because $P > 0$, there exist $c_1 > 0$ and $c_2 > 0$ such that

$$c_1\|x-x^*\|^2 \le V(x) \le c_2\|x-x^*\|^2 \tag{7}$$

holds. The derivatives of $V(x)$ along the trajectories of (1) and (2) are

$$\begin{aligned}\alpha_1(x) :&= \frac{\partial V}{\partial x}(A_1x+B_1u_0)\\ &= (x-x^*)^T\left(PA_1+A_1^TP\right)(x-x^*)\\ &\quad +2(A_1x^*+B_1u_0)^TP(x-x^*),\end{aligned} \tag{8}$$

$$\begin{aligned}\alpha_2(x) :&= \frac{\partial V}{\partial x}(A_2x+B_2u_0)\\ &= (x-x^*)^T\left(PA_2+A_2^TP\right)(x-x^*)\\ &\quad +2(A_2x^*+B_2u_0)^TP(x-x^*),\end{aligned} \tag{9}$$

respectively.

Proposition 2. *Suppose that* $PA_1+A_1^TP \le 0$ *and* $PA_2+A_2^TP \le 0$. *Then,*

$$\alpha_2^{(-1)}(\mathbb{R}_{(\ge 0)}) \subset \alpha_1^{(-1)}(\mathbb{R}_{(\le 0)}),\ \alpha_1^{(-1)}(\mathbb{R}_{(\ge 0)}) \subset \alpha_2^{(-1)}(\mathbb{R}_{\le 0}), \tag{10}$$

$$\begin{aligned}\alpha_1^{-1}(0)\cap\alpha_2^{-1}(0) = \Big\{x : x-x^* \in \ker\left(PA_1+A_1^TP\right)\\ \cap\ker\left(PA_2+A_2^TP\right),\cap\ker(A_1x^*+B_1u_0)^TP\Big\}.\end{aligned} \tag{11}$$

The proof is based on the following observation.

Lemma 1. *Let* $Q_1 \le 0$ *and* $Q_2 \le 0$ *be* $n\times n$ *symmetric matrices. Let* $v_1 \in \mathbb{R}^n$ *and* $v_2 \in \mathbb{R}^n$ *satisfy* $\lambda v_1 + (1-\lambda)v_2 = 0$ *for some* $0 < \lambda < 1$. *Define*

$$p_1(x) := x^TQ_1x + v_1^Tx, \quad p_2(x) := x^TQ_2x + v_2^Tx.$$

Then

$$\begin{aligned}&p_1^{-1}(\mathbb{R}_{\le 0}) \subset p_2^{-1}(\mathbb{R}_{\ge 0}), \quad p_2^{-1}(\mathbb{R}_{\le 0}) \subset p_1^{-1}(\mathbb{R}_{\ge 0}),\\ &p_1^{-1}(0)\cap p_2^{-1}(0) = \ker Q_1 \cap \ker Q_2 \cap \ker v_1^T.\end{aligned}$$

Proof. If $p_1(x) > 0$, then

$$\begin{aligned}0 < \lambda p_1(x) &= \lambda x^TQ_1x + \lambda v_1^Tx\\ &\le \lambda v_1^Tx = -(1-\lambda)v_2^Tx\\ &\le -(1-\lambda)x^TQ_2x - (1-\lambda)v_2^Tx = -(1-\lambda)p_2(x)\end{aligned}$$

holds. Thus, $p_2(x) < 0$. Because $p_1^{-1}(\mathbb{R}_{\le 0}) = \mathbb{R}^n \setminus p_1^{-1}(\mathbb{R}_{>0})$ and $p_2^{-1}(\mathbb{R}_{\ge 0}) = \mathbb{R}^n \setminus p_2^{-1}(\mathbb{R}_{<0})$, $p_2^{-1}(\mathbb{R}_{\ge 0}) \subset p_1^{-1}(\mathbb{R}_{\le 0})$. By interchanging p_1 and p_2, in the argument, it follows that $p_1^{-1}(\mathbb{R}_{\ge 0}) \subset p_2^{-1}(\mathbb{R}_{\le 0})$. If $p_1(x) = p_2(x) = 0$, then

$$\begin{aligned}0 = \lambda p_1(x) &= \lambda x^TQ_1x + \lambda v_1^Tx\\ &\le \lambda v_1^Tx = -(1-\lambda)v_2^Tx\\ &\le -(1-\lambda)x^TQ_2x - (1-\lambda)v_2^Tx = -(1-\lambda)p_2(x) = 0.\end{aligned}$$

Hence all the inequalities hold as equalities. This implies $v_1^Tx = 0$, $x^TQ_1x = 0$, and $x^TQ_2x = 0$, which means $x \in \ker Q_1 \cap \ker Q_2 \cap \ker v_1^T$. Conversely, if $x \in \ker Q_1 \cap \ker Q_2 \cap \ker v_1^T$, then $x \in \ker v_2^T$ and $p_1(x) = p_2(x) = 0$. □

Proof of Proposition 2. Define

$$\begin{aligned}&Q_1 := PA_1 + A_1^TP, \quad Q_2 := PA_2 + A_2^TP,\\ &v_1 := 2P(A_1x^* + B_1u_0), \quad v_2 := 2P(A_2x^* + B_2u_0),\\ &p_1(x) := \alpha_1(x+x^*), \quad p_2(x) := \alpha_2(x+x^*).\end{aligned}$$

Notice that the assumptions of Lemma 1 are satisfied since (5) holds. Then the proof is immediate from Lemma 1. □

Based on Proposition 2, we propose the following switching control mechanism.

Switching Mechanism A

- If the system is operating in mode 1 and reaches $\alpha_1^{-1}(0)$, then it switches to mode 2.
- If the system is operating in mode 2 and reaches $\alpha_2^{-1}(0)$, then it switches to mode 1.

Remark 1. Switching Mechanism A is initially proposed for a boost converter model in [32]. Proposition 2 clarifies a condition that ensures that Switching Mechanism A is well defined.

To analyse the stability of the switching control law, we consider the differential inclusion

$$\frac{dx}{dt} \in F(x), \tag{12}$$

$$F(x) := \begin{cases}\{A_1x+B_1u_0\} & \text{if } x \in M_1,\\ \{A_2x+B_2u_0\} & \text{if } x \in M_2,\\ \operatorname{conv}\{A_1x+B_1u_0,\ A_2x+B_2u_0\} & \text{if } x \in M_0,\end{cases}$$

where

$$\begin{aligned}M_1 &= \left\{x : \alpha_1^{-1}(\mathbb{R}_{<0}) \cap \alpha_1^{-1}(\mathbb{R}_{>0}) = \alpha_1^{-1}(\mathbb{R}_{<0})\right\},\\ M_2 &= \left\{x : \alpha_1^{-1}(\mathbb{R}_{>0}) \cap \alpha_2^{-1}(\mathbb{R}_{<0}) = \alpha_2^{-1}(\mathbb{R}_{<0})\right\},\\ M_0 &= \left\{x : \alpha_1^{-1}(\mathbb{R}_{\le 0}) \cap \alpha_2^{-1}(\mathbb{R}_{\le 0})\right\}.\end{aligned}$$

The set-valued map $F : \mathbb{R}^n \to \mathbb{R}^n$ is upper semi-continuous, and its values are bounded closed convex sets. Solutions of (12) include solutions of (1), (2) with the switching control mechanism. We shall analyse the stability of the operating point x^* of the differential inclusion (12).

Remark 2. The switching mechanism that selects the mode defined by

$$\arg\min\{\alpha_i(x) : i = 1, 2\}$$

is in line with the method used in [29], except that [29] assumes that

$$P(\lambda A_1 + (1-\lambda)A_2) + (\lambda A_1 + (1-\lambda)A_2)^T P < 0$$

for some $\lambda \in (0, 1)$. This mechanism does not stabilize the operating point asymptotically when we only assume $PA_1 + A_1^T P \leq 0$ and $PA_2 + A_2^T P \leq 0$. The following simple example

$$A_1 = \begin{bmatrix} 0 & 0 \\ 0 & -1 \end{bmatrix}, B_1 = \begin{bmatrix} 0 \\ 0 \end{bmatrix}, A_2 = \begin{bmatrix} 0 & 1 \\ -1 & -1 \end{bmatrix}, B_1 = \begin{bmatrix} 0 \\ 0 \end{bmatrix},$$

$$P = \begin{bmatrix} 1 & 0 \\ 0 & 1 \end{bmatrix}$$

results in the differential inclusion

$$\frac{dx}{dt} \in F(x),$$

$$F(x) = \begin{cases} \{1\} & \text{if } [0\ 1]\, x \neq 0, \\ \{1, 2\} & \text{if } [0\ 1]\, x = 0. \end{cases}$$

If $[0\ 1]\, x_0 = 0$, then the differential inclusion has the unique solution $x(t) \equiv x_0$, which shows that it is not asymptotically stable. Note that this is not a counterexample of [29, Theorem 2]. Nevertheless, the example shows that the distinction of positive definiteness and positive semi-definiteness is meaningful.

3 | STABILITY OF SWITCHING SYSTEM

In this section, we analyse the stability of the switching mechanism proposed in the previous section and apply the method to a DC–DC zeta converter operating in the CCM.

3.1 | Stability analysis

Consider the differential inclusion (12) and the function $V(x)$ in (6). Define $\dot{V}(x) : \mathbb{R}^n \to \mathbb{R}$ by

$$\dot{V}(x) = \frac{\partial V}{\partial x} F(x) := \left\{ \frac{\partial V}{\partial x}\omega : \omega \in F(x) \right\}.$$

It is easy to verify that

$$\dot{V}(x) = \begin{cases} \{\alpha_1(x)\} & \text{if } x \in M_1, \\ \{\alpha_2(x)\} & \text{if } x \in M_2, \\ \text{conv}\,\{\alpha_1(x), \alpha_2(x)\} & \text{if } x \in M_0. \end{cases} \tag{13}$$

The inverse image $\dot{V}^{-1}(S)$, where $S \subset \mathbb{R}$, is defined by

$$\dot{V}^{-1}(S) := \left\{ y \in \mathbb{R}^n : \dot{V}(y) \cap S \neq \emptyset \right\}.$$

When $S = \{a\}$, we write $\dot{V}^{-1}(a) := \dot{V}^{-1}(\{a\})$.

Proposition 3. *Consider the differential inclusion (12) and the Lyapunov function (6). Then,*

$$\dot{V}^{-1}(0) = \alpha_1^{-1}(0) \cup \alpha_2^{-1}(0).$$

Proof. If $x \in \alpha_1^{-1}(0)$, then $\dot{V}(x) = \text{conv}\,\{0, \alpha_2(x)\} \ni 0$. Similarly, we have $0 \in \dot{V}(x)$ if $x \in \alpha_2^{-1}(0)$. Hence $\dot{V}^{-1}(0) \supset \alpha_1^{-1}(0) \cup \alpha_2^{-1}(0)$. Conversely, if $0 \in \dot{V}(x)$, then $x \in \alpha_1^{-1}(\mathbb{R}_{\leq 0}) \cap \alpha_2^{-1}(\mathbb{R}_{\leq 0})$ and $0 \in \text{conv}\,\{\alpha_1(x), \alpha_2(x)\}$. Because $\alpha_1(x) \leq 0$ and $\alpha_2(x) \leq 0$, this implies either $\alpha_1(x) = 0$ or $\alpha_2(x) = 0$. □

Proposition 4. *Let x^*, S_1, and S_2 be defined by (3) and (4). Then $\{x^*\} \cup S_1 \subset \alpha_2^{-1}(0)$ holds.*

Proof. We have already shown that $x^* \in \alpha_1^{-1}(0) \cap \alpha_2^{-1}(0)$ in Proposition 2. If $x \in S_1$, then $\alpha_1(x) = 0$ by (8). Similarly, if $x \in S_2$, then $\alpha_2(x) = 0$. □

Proposition 5. *Let $x^\# \in \{x^*\} \cup S_1 \cup S_2$. Then, the differential inclusion (12) has a stationary solution $\phi(t, x^\#) \equiv x^\#$.*

Proof. If $x^\# \in S_1$, then $\alpha_1(x^\#) = 0$ by Proposition 4. Thus $F(x^\#) = \text{conv}\,\{0, A_2 x^{*1} + B_2 u_0\} \ni 0$. Similarly, $x^\# \in S_2$ implies $0 \in F(x^\#)$. By Proposition 4, $\alpha_1(x^*) = \alpha_2(x^*) = 0$. Consequently, $F(x^*) = \text{conv}\,\{A_1 x^* + B_1 u_0, A_2 x^* + B_2 u_0\} \ni \lambda(A_1 x^* + B_1 u_0) + (1-\lambda)(A_2 x^* + B_2 u_0) = 0$. □

By Proposition 5, the operation point x^* is not globally asymptotically stable if $S_1 \cup S_2 \neq \emptyset$. We shall study the local asymptotic stability of x^*. The next result shows that x^* is stable in this sense.

Theorem 1. *Suppose that $PA_1 + A_1^T P \leq 0$ and $PA_2 + A_2^T P \leq 0$ hold. If $\alpha_1^{-1}(0) \cap \alpha_2^{-1}(0)$ contains no solution of (12) except for $x(t) \equiv x^*$, then x^* is locally asymptotically stable.*

The proof of Theorem 1 hinges on a couple of Lemmas. The first one states that the operating point x^* is stable.

Lemma 2. *Suppose that $PA_1 + A_1^T P \leq 0$ and $PA_2 + A_2^T P \leq 0$ hold. Then x^* is stable.*

Proof. Note that the set-valued function $F(x)$ in (12) is defined for all $x \in \mathbb{R}^n$ from (10) in Proposition 2. Let $\varepsilon > 0$, and choose $\delta = \frac{\varepsilon c_1}{c_2} > 0$. If $\|x_0 - x^*\|^2 < \delta$, it follows from (7) that $V(x_0) \leq c_2\delta = c_1\,\varepsilon$. Along the trajectory $\phi(t, x_0)$ of

(12), it holds that

$$\frac{d}{dt}V\ \left(\phi\left(t,x_0\right)\right)=\dot{V}\ \left(\phi\left(t,x_0\right)\right)\subset\mathbb{R}_{\le 0},$$

by (13), and hence $V(\phi(t,x_0))\le V(x_0)$ holds. This implies that $\|\phi(t,x_0)-x^*\|^2\le\varepsilon$, and therefore x^* is stable. □

One of the important observations is the property of the limiting set of a solution of a differential inclusion with an upper semi-continuous set-valued map. Let

$$\frac{dx}{dt}\in F\left(x\right), \tag{14}$$

be a differential inclusion where $F:\ \mathbb{R}^n\to\mathbb{R}^n$ is upper semi-continuous and its values are bounded closed convex sets. Let $\phi(t,x_0)$ be a solution of (14). A point $\omega\in\mathbb{R}^n$ is called a limit point of $\phi(t,x_0)$ if there is a sequence $\{t_k\}$ in $[0,\ \infty)$ such that $t_k\to\infty$ and

$$\lim_{k\to\infty}\phi\left(t_k,x_0\right)=\ \omega.$$

The set of all limit points of $\phi(t,x_0)$ is called the limit set of $\phi(t,x_0)$ and is denoted as Ω.

Lemma 3. *Consider the differential inclusion (14). Suppose that a solution $\phi(t,x_0)$ is bounded. Then the limit set Ω is non-empty, closed, and bounded. Furthermore, if $\omega\in\Omega$, then there exists a solution of $\phi(t,\omega)$ of (14) with initial condition $x\ (0)=\ \omega$ satisfying $\phi(t,\omega)\in\Omega$ for all $t\ge 0$.*

Proof. The first half is elementary, see for example [33, Lemma 5.30]. To prove the second half, let $\{t_k\}$ be a sequence in $[0,\infty)$ such that $t_k\to\infty$ and $\omega_k:=\phi(t_k,x_0)$ tends to $\omega\in\Omega$. Let $T>0$ be fixed, and define $\psi_k(t):=\phi(t+t_k,x_0)$ for $t\in[0,T]$. Note that $\psi_k(t)$ is a solution of (14) with the initial condition $x\ (0)=\omega_k$. Using a similar argument as in [34, p.13, Theorem 4] and [34, p.104, Theorem 1], one can prove there exists ψ and a convergent subsequence of $\{\psi_k\}$ where limit is ψ, and $\psi\ (t)=\ \phi(t,\omega)$ is a solution of the differential inclusion (14) with the initial condition $x\ (0)=\ \omega$. Then any point on $\psi(t)$ is a limit point of $\phi(t,x_0)$ and hence $\phi(t,\omega)\in\Omega$ for $0\le t\le T$. Since this is true for any $T>0$, this concludes the proof. □

Lemma 4. *There exists $r>0$ such that for every ω in the set $\{(\alpha_1^{-1}(0)\setminus\alpha_2^{-1}(0))\cup(\alpha_2^{-1}(0)\setminus\alpha_1^{-1}(0))\}\cap\{x:V(x)<r\}$ and every solution $\phi(t,\omega)$ of (12), there exists $\tau>0$ such that $V(\phi(\tau,\omega))<V(\omega)$.*

Proof. Define

$$\dot{\alpha}_1\left(x\right):=\frac{\partial\alpha_1\left(x\right)}{\partial x}\left(A_1x+B_1u_0\right),$$

and recall from (9) that

$$\frac{\partial\alpha_1\left(x\right)}{\partial x}=\ 2\left(\left(x-x^*\right)^T\ \left(PA_1+A_1^TP\right)+\left(A_1x^*+B_1u_0\right)^TP\right).$$

It follows that $\dot{\alpha}_1(x)$ is a continuous function; moreover,

$$\dot{\alpha}_1\ \left(x^*\right)=\left(A_1x^*+B_1u_0\right)^T\ P\left(A_1x^*+B_1u_0\right)>0,$$

and from the continuity of $\dot{\alpha}_1(x)$, $\dot{\alpha}_1(x)>0$ in some neighbourhood of x^*, say $N\ =\{x:V(x)<r\}$ for some $r>0$. Let $\omega\in(\alpha_1^{-1}(0)\setminus\alpha_2^{-1}(0))\cap N$. Since $\alpha_1\ (\omega)=\ 0,\alpha_2(\omega)<0$ by (10). We can take $\tau>0$ small enough, so $\alpha_2(\phi(\tau,\omega))<0$ for all $t\in[0,\tau]$. If $V\ (\phi(t,\omega))=\ V(\omega)$ for all $t\in[0,\tau]$, then

$$\frac{d}{dt}V\ \left(\phi\left(t,\omega\right)\right)=\frac{\partial V}{\partial x}\ \frac{d}{dt}\phi\ \left(t,\omega\right)=0, \tag{15}$$

for almost all t. Let $\mathcal{T}=\{t:\alpha_1(\phi(\tau,\omega))>0\}$. Note that $\mathcal{T}$ is an open set. If $t\in\mathcal{T}$, then by (12) $F(\phi(\tau,\omega))=\{A_2\phi(\tau,\omega)+B_2u_0\}$, and hence $\frac{\partial V}{\partial x}\frac{d}{dt}\phi(t,\omega)=\alpha_2(\phi(\tau,\omega))<0$. Hence $\mathcal{T}=\emptyset$. Consequently, $F(\phi(\tau,\omega))=\operatorname{conv}\{A_1\phi(\tau,\omega)+B_1u_0,A_2\phi(\tau,\omega)+B_2u_0\}$, but $\frac{\partial V}{\partial x}A_2\phi(\tau,\omega)+B_2u_0=\alpha_2(\phi(\tau,\omega))<0$ implies $\frac{d}{dt}\phi(\tau,\omega)=A_1\phi(\tau,\omega)+B_1u_0$ for almost all t. Hence $\phi(\tau,\omega)$ is the solution of the differential equation

$$\frac{dx}{dt}=A_1\ x+B_1u_0,\ x\ (0)=\ \omega,\ 0\le t\le\tau,$$

$V(\phi(t,\omega))$ is twice continuously differentiable, and

$$\frac{d^2}{dt^2}V\ \left(\phi\left(t,\omega\right)\right)=\dot{\alpha}_1\ \left(\phi\left(t,\omega\right)\right)>0,\ t\in\left[0,\tau\right].$$

This implies that $\alpha(\phi(t,\omega))>\alpha\ (\phi(0,\omega))=\ 0$ for some t. But $\mathcal{T}\ =\ \emptyset$, and this is not possible. Hence, $V(\phi(\tau,\omega))\le V(\phi(t,\omega))<V(\omega)$ for some $t\in[0,\tau]$. The proof for $\omega\in(\alpha_2^{-1}(0)\setminus\alpha_1^{-1}(0))\cap N$ is similar. □

Proof of Theorem 1. Since $\phi(t,x_0)$ is bounded, its limit set Ω is an invariant set by Lemma 3. Since $V(x)$ is bounded from below and $V(\phi(t,x_0))$ is monotonically non-increasing for every sequence $\{t_k\}$ such that $t_k\to\infty$ as $k\to\infty$, $c:=\lim_{k\to\infty}V(\phi(t_k,x_0))$ exists. If $\omega\in\Omega$, then there exists a sequence $\{t_k\}$ such that $\omega\ =\ \lim\phi(t_k,x_0)$. This means $V\ (\omega)=V\ (\lim\phi(t_k,x_0))=\lim V(\phi(t_k,x_0))\ =\ c$. Because Ω is an invariant set, $0\in V(\omega)$ for any $\omega\in\Omega$. From Proposition 3, $\omega\in\alpha_1^{-1}(0)\cup\alpha_2^{-1}(0)$. Take $r>0$ and $N\ =\{x:V(x)<r\}$ as in Lemma 4. If $\omega\in\{(\alpha_1^{-1}(0)\setminus\alpha_2^{-1}(0))\cup(\alpha_2^{-1}(0)\setminus\alpha_1^{-1}(0))\}\cap N$, then ω is not a limit point by Lemma 4. Thus, $\omega\in\alpha_1^{-1}(0)\cap\alpha_2^{-1}(0)$. Hence, if $V(x_0)<r$, then $\phi(t,x_0)$ does not have a limit point except x^*. □

Remark 3. Theorem 1 is a consequence of LaSalle's invariance principle proved for the differential inclusion (12). This is a useful tool to prove the stability of the switching control applied to a DC–DC zeta converter in Section 3.2.

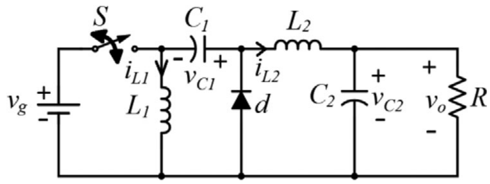

FIGURE 1 A DC–DC zeta converter circuit

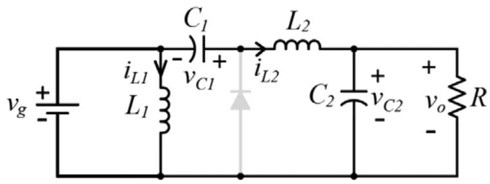

FIGURE 2 Equivalent circuit when the switch is closed

3.2 | DC–DC zeta converter operating in continuous conduction mode

Consider the DC–DC zeta converter circuit shown in Figure 1. The circuit consists of two inductors L_1 and L_2, two capacitors C_1 and C_2, an ideal diode d and C_2, a DC voltage source v_g, a resistive load R, and an ideal switch S. Denote the currents of L_1 and L_2 as i_{L1} and i_{L2}, the voltages of C_1 and C_2 as v_{C1} and v_{C2}, respectively.

The converter is in CCM if the diode d is open when the switch S is on and it is shorted when the switch is off. When the switch is closed (mode 1), the converter is equivalent to the circuit shown in Figure 2, and when the switch is open (mode 2), the converter is equivalent to the circuit shown in Figure 3. With the state vector $x = [i_{L1}\ i_{L2}\ v_{C1}\ v_{C2}]^T$ and the input $u = v_g$, the matrices for the two modes are given by

$$A_1 = \begin{bmatrix} 0 & 0 & 0 & 0 \\ 0 & 0 & \frac{1}{L_2} & -\frac{1}{L_2} \\ 0 & -\frac{1}{C_1} & 0 & 0 \\ 0 & \frac{1}{C_2} & 0 & -\frac{1}{RC_2} \end{bmatrix}, \quad B_1 = \begin{bmatrix} \frac{1}{L_1} \\ \frac{1}{L_2} \\ 0 \\ 0 \end{bmatrix},$$

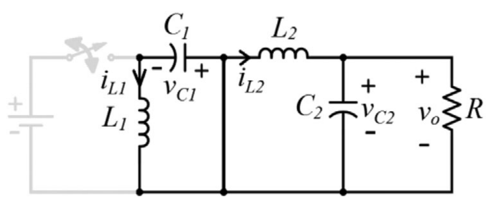

FIGURE 3 Equivalent circuit when the switch is open

$$A_2 = \begin{bmatrix} 0 & 0 & -\frac{1}{L_1} & 0 \\ 0 & 0 & 0 & -\frac{1}{L_2} \\ \frac{1}{C_1} & 0 & 0 & 0 \\ 0 & \frac{1}{C_2} & 0 & -\frac{1}{RC_2} \end{bmatrix}, \quad B_2 = \begin{bmatrix} 0 \\ 0 \\ 0 \\ 0 \end{bmatrix}. \tag{16}$$

If $u_0 > 0$, then mode 1 has no stationary solution, and mode 2 has a unique stationary solution $x^{*2} = [0\ 0\ 0\ 0]^T$.

For $\lambda \in (0, 1)$,

$$x^* = -(\lambda A_1 + (1-\lambda) A_2)^{-1} (\lambda B_1 + (1-\lambda) B_2) u_0$$

$$= \begin{bmatrix} 0 & 0 & -\frac{1-\lambda}{L_1} & 0 \\ 0 & 0 & \frac{\lambda}{L_2} & -\frac{1}{L_2} \\ \frac{1-\lambda}{C_1} & -\frac{\lambda}{C_1} & 0 & 0 \\ 0 & \frac{1}{C_2} & 0 & -\frac{1}{RC_2} \end{bmatrix} \begin{bmatrix} \frac{\lambda}{L_1} \\ \frac{\lambda}{L_2} \\ 0 \\ 0 \end{bmatrix} u_0$$

$$= \begin{bmatrix} \frac{v_r^2}{Rv_g} \\ \frac{v_r}{R} \\ v_r \\ v_r \end{bmatrix} =: \begin{bmatrix} i_{L1}^* \\ i_{L2}^* \\ v_{C1}^* \\ v_{C2}^* \end{bmatrix}, \tag{17}$$

where $v_g := u_0$ and $v_r := \frac{\lambda u_0}{1-\lambda}$. Based on the energy stored in the zeta converter, define

$$P := \begin{bmatrix} \frac{L_1}{2} & 0 & 0 & 0 \\ 0 & \frac{L_2}{2} & 0 & 0 \\ 0 & 0 & \frac{C_1}{2} & 0 \\ 0 & 0 & 0 & \frac{C_2}{2} \end{bmatrix}. \tag{18}$$

Then

$$PA_1 + A_1^T P = \begin{bmatrix} 0 & 0 & 0 & 0 \\ 0 & 0 & 0 & 0 \\ 0 & 0 & 0 & 0 \\ 0 & 0 & 0 & -\frac{1}{R} \end{bmatrix} \leq 0,$$

$$PA_2 + A_2^T P = \begin{bmatrix} 0 & 0 & 0 & 0 \\ 0 & 0 & 0 & 0 \\ 0 & 0 & 0 & 0 \\ 0 & 0 & 0 & -\frac{1}{R} \end{bmatrix} \le 0,$$

$$(A_1x^* + B_1u_0)^T P = \begin{bmatrix} \frac{v_g}{2} & \frac{v_g}{2} & -\frac{v_r}{2R} & 0 \end{bmatrix},$$

$$(A_2x^* + B_2u_0)^T P = \begin{bmatrix} -\frac{v_r}{2} & -\frac{v_r}{2} & -\frac{v_r^2}{2Rv_g} & 0 \end{bmatrix}. \quad (19)$$

From (19), $\ker\,(PA_1 + A_1^T P) \cap \ker\,(PA_2 + A_2^T P) \cap \ker\,(A_1x^* + B_1u_0)^T P = \operatorname{span}\{d_1, d_2\}$ where

$$d_1 = \begin{bmatrix} \frac{v_r}{R} \\ 0 \\ v_g \\ 0 \end{bmatrix}, \quad d_2 = \begin{bmatrix} 0 \\ \frac{v_r}{R} \\ v_g \\ 0 \end{bmatrix}. \quad (20)$$

The function $V(x)$ decreases along the trajectory as long as $x \notin \alpha_1^{-1}(0) \cap \alpha_2^{-1}(0)$. It remains to see what happens when the trajectory reaches $\alpha_1^{-1}(0) \cap \alpha_2^{-1}(0)$.

Lemma 5. *Let $x \in \alpha_1^{-1}(0) \cap \alpha_2^{-1}(0)$. Then the following properties hold:*

a. $0 \in F(x)$ *if and only if* $x = x^*$.
b. *If* $x - x^* \notin \operatorname{span}\{d_1\}$, *then* $F(x) \cap \ker\,(PA_1 + A_1^T P) \cap \ker\,(PA_2 + A_2^T P) \neq \emptyset$.
c. *If* $x - x^* \in \operatorname{span}\{d_1\}$, *and* $x \neq x^*$, *then* $F(x) \cap \operatorname{span}\{d_1\} \neq \emptyset$.

Proof. It follows from (17) that

$$A_1x^* + B_1\,v_g = \begin{bmatrix} 0 \\ 0 \\ -\frac{v_r}{C_1R} \\ 0 \end{bmatrix} + \begin{bmatrix} \frac{v_g}{L_1} \\ \frac{v_g}{L_2} \\ 0 \\ 0 \end{bmatrix} = \begin{bmatrix} \frac{v_g}{L_1} \\ \frac{v_g}{L_2} \\ -\frac{v_r}{C_1R} \\ 0 \end{bmatrix}, \quad (21)$$

$$A_2x^* + B_2\,v_g = \begin{bmatrix} -\frac{v_r}{L_1} \\ -\frac{v_r}{L_2} \\ \frac{v_r^2}{C_1Rv_g} \\ 0 \end{bmatrix} + \begin{bmatrix} 0 \\ 0 \\ 0 \\ 0 \end{bmatrix} = \begin{bmatrix} -\frac{v_r}{L_1} \\ -\frac{v_r}{L_2} \\ \frac{v_r^2}{C_1Rv_g} \\ 0 \end{bmatrix}. \quad (22)$$

Note that $x \in \alpha_1^{-1}(0) \cap \alpha_2^{-1}(0)$ if and only if $x = x^* + \Delta x$ with

$$\Delta x = \delta_1\,d_1 + \delta_2\,d_2 = \begin{bmatrix} \delta_1\frac{v_r}{R} \\ \delta_2\frac{v_r}{R} \\ (\delta_1 + \delta_2)\,v_g \\ 0 \end{bmatrix}. \quad (23)$$

From this, it follows that

$$A_1\Delta x = \begin{bmatrix} 0 \\ (\delta_1 + \delta_2)\frac{v_g}{L_2} \\ -\delta_2\frac{v_r}{C_1R} \\ \delta_2\frac{v_r}{C_2R} \end{bmatrix}, \quad A_2\Delta x = \begin{bmatrix} -(\delta_1 + \delta_2)\frac{v_g}{L_1} \\ 0 \\ \delta_1\frac{v_r}{C_1R} \\ \delta_2\frac{v_r}{C_2R} \end{bmatrix}.$$

Hence if $x \in \alpha_1^{-1}(0) \cap \alpha_2^{-1}(0)$, then

$$A_1x + B_1\,v_g = A_1\,x^* + B_1v_g + A_1\Delta x$$

$$= \begin{bmatrix} \frac{v_g}{L_1} \\ \frac{v_g}{L_2} \\ -\frac{v_r}{C_1R} \\ 0 \end{bmatrix} + \begin{bmatrix} 0 \\ (\delta_1 + \delta_2)\frac{v_g}{L_2} \\ -\delta_2\frac{v_r}{C_1R} \\ \delta_2\frac{v_r}{C_2R} \end{bmatrix}, \quad (24)$$

$$A_2x + B_2\,v_g = A_2\,x^* + B_2v_g + A_2\Delta x$$

$$= \begin{bmatrix} -\frac{v_r}{L_1} \\ -\frac{v_r}{L_2} \\ \frac{v_r^2}{C_1Rv_g} \\ 0 \end{bmatrix} + \begin{bmatrix} -(\delta_1 + \delta_2)\frac{v_g}{L_1} \\ 0 \\ \delta_1\frac{v_r}{C_1R} \\ \delta_2\frac{v_r}{C_2R} \end{bmatrix}. \quad (25)$$

Hence if $\omega \in F(x)$ for $x \in \alpha_1^{-1}(0) \cap \alpha_2^{-1}(0) \setminus \operatorname{span}\{d_1\}$, then

$$[0 \quad 0 \quad 0 \quad 1]\,\omega = \frac{\delta_2 v_r}{C_2R} \neq 0,$$

which shows $F(x) \cap \ker\,(PA_1 + A_1^T P) \cap \ker\,(PA_2 + A_2^T P) \neq \emptyset$ and $0 \notin \operatorname{conv}\{A_1x + B_1v_g, A_2x + B_2v_g\}$. Suppose $x - x^* \in \operatorname{span}\{d_1\}$, then,

$$\operatorname{rank}\,\left[\,(A_1x + B_1v_g)\;\;(A_2x + B_2v_g)\,\right]$$

$$
= \operatorname{rank}\begin{bmatrix} \frac{v_g}{L_1} & -\frac{v_r}{L_1} - \delta_1 \frac{v_g}{L_1} \\ \frac{v_g}{L_2} + \delta_1 \frac{v_g}{L_2} & -\frac{v_r}{L_2} \\ -\frac{v_r}{C_1 R} & \frac{v_r^2}{C_1 R v_g} + \delta_1 \frac{v_r}{C_1 R} \end{bmatrix}
$$

$$
= \operatorname{rank}\begin{bmatrix} \frac{v_g}{L_1} & -\delta_1 \frac{v_g}{L_1} \\ \frac{v_g}{L_2} + \delta_1 \frac{v_g}{L_2} & \delta_1 \frac{v_r}{L_2} \\ -\frac{v_r}{C_1 R} & \delta_1 \frac{v_r}{C_1 R} \end{bmatrix}
$$

$$
= \operatorname{rank}\begin{bmatrix} \frac{v_g}{L_1} & -\frac{v_g}{L_1} \\ \frac{v_g}{L_2} + \delta_1 \frac{v_g}{L_2} & \frac{v_r}{L_2} \\ -\frac{v_r}{C_1 R} & \frac{v_r}{C_1 R} \end{bmatrix}
$$

$$
= \operatorname{rank}\begin{bmatrix} 0 & -\frac{v_g}{L_1} \\ \frac{v_r+v_g}{L_2} + \delta_1 \frac{v_g}{L_2} & \frac{v_r}{L_2} \\ 0 & \frac{v_r}{C_1 R} \end{bmatrix}.
$$

If $\delta_1 \neq -\frac{v_r+v_g}{v_g}$, then $A_1x + B_1v_g$ and $A_2x + B_2v_g$ are linearly independent, and hence $0 \notin F(x)$. If $\delta_1 = -\frac{v_r+v_g}{v_g}$, then

$$
x = x^* + \Delta x = \begin{bmatrix} \frac{v_r^2}{R v_g} \\ \frac{v_r}{R} \\ v_r \\ v_r \end{bmatrix} + \begin{bmatrix} -\frac{v_r+v_g}{v_g}\left(\frac{v_r}{R}\right) \\ 0 \\ -\frac{v_r+v_g}{v_g}\left(v_g\right) \\ 0 \end{bmatrix} = \begin{bmatrix} -\frac{v_r}{R} \\ \frac{v_r}{R} \\ -v_g \\ v_r \end{bmatrix},
$$

$$
A_1x + B_1\, v_g = \begin{bmatrix} \frac{v_g}{L_1} \\ \frac{v_g}{L_2} \\ -\frac{v_r}{C_1 R} \\ 0 \end{bmatrix} + \begin{bmatrix} 0 \\ -\frac{v_r+v_g}{v_g}\left(\frac{v_g}{L_2}\right) \\ 0 \\ 0 \end{bmatrix} = \begin{bmatrix} \frac{v_g}{L_1} \\ -\frac{v_r}{L_2} \\ -\frac{v_r}{C_1 R} \\ 0 \end{bmatrix},
$$

$$
A_2x + B_2\, v_g = \begin{bmatrix} -\frac{v_r}{L_1} \\ -\frac{v_r}{L_2} \\ \frac{v_r^2}{C_1 R v_g} \\ 0 \end{bmatrix} + \begin{bmatrix} \frac{v_r+v_g}{v_g}\left(\frac{v_g}{L_1}\right) \\ 0 \\ -\frac{v_r+v_g}{v_g}\left(\frac{v_r}{C_1 R}\right) \\ 0 \end{bmatrix} = \begin{bmatrix} \frac{v_g}{L_1} \\ -\frac{v_r}{L_2} \\ -\frac{v_r}{C_1 R} \\ 0 \end{bmatrix}.
$$

Because $A_1x + B_1\, v_g = A_2\, x + B_2v_g \neq 0$, we have $0 \notin F(x)$. Finally, note that $\Delta x^T P(A_1x + B_1v_g)$

$$
= \begin{bmatrix} \delta_1 \frac{L_1 v_r}{2R} & \delta_2 \frac{L_2 v_r}{2R} & (\delta_1+\delta_2)\frac{C_1 v_g}{2} & 0 \end{bmatrix} \left\{ \begin{bmatrix} \frac{v_g}{L_1} \\ \frac{v_g}{L_2} \\ -\frac{v_r}{C_1 R} \\ 0 \end{bmatrix} + \begin{bmatrix} 0 \\ (\delta_1+\delta_2)\frac{v_g}{L_2} \\ -\delta_2 \frac{v_r}{C_1 R} \\ \delta_2 \frac{v_r}{C_2 R} \end{bmatrix} \right\}
$$

$$
= 0,
$$

$$
\Delta x^T P\left(A_2 x + B_2 v_g\right)
$$

$$
= \begin{bmatrix} \delta_1 \frac{L_1 v_r}{2R} & \delta_2 \frac{L_2 v_r}{2R} & (\delta_1+\delta_2)\frac{C_1 v_g}{2} & 0 \end{bmatrix} \left\{ \begin{bmatrix} \frac{v_r}{L_1} \\ \frac{v_r}{L_2} \\ -\frac{v_r}{C_1 R v_g} \\ 0 \end{bmatrix} + \begin{bmatrix} -(\delta_1+\delta_2)\frac{v_g}{L_1} \\ 0 \\ \delta_1 \frac{v_r}{C_1 R} \\ \delta_2 \frac{v_r}{C_2 R} \end{bmatrix} \right\}
$$

$$
= 0.
$$

Let $x - x^* \in \operatorname{span}\{d_1\}$ and $x \neq x^*$. Then for every $\omega \in F(x)$, $d_1^T P\omega = 0$. Since $0 \notin F(x)$, it follows that $F(x) \cap \operatorname{span}\{d_1\} = \emptyset$. □

Theorem 2. *Consider the differential inclusion (12) defined by the system matrices (16) and the operating point x^* in (17). Then, the operating point x^* is local asymptotically stable.*

Proof. Assume that $\phi(t, x_0)$ is a solution of the differential inclusion satisfying $\phi(t, x_0) \in \alpha_1^{-1}(0) \cap \alpha_2^{-1}(0)$ for $t \geq 0$ and $x_0 \neq x^*$. If $x_0 - x^* \notin \operatorname{span}\{d_1\}$, then $\frac{d}{dt}\phi(t, x_0) \notin \ker\,(PA_1 + A_1^T P) \cap \ker\,(PA_2 + A_2^T P)$ by Lemma 5, but this contradicts the assumption that $\phi(t, x_0) \in \alpha_1^{-1}(0) \cap \alpha_2^{-1}(0)$ for $t \geq 0$. If $x_0 - x^* \in \operatorname{span}\{d_1\}$, then from Lemma 5, there exists t_1 such that $x_1 := \phi(t_1, x_0)$ satisfies $x_1 - x^* \notin \operatorname{span}\{d_1\}$. Then the trajectory $\phi(t, x_1)$ cannot stay in $\alpha_1^{-1}(0) \cap \alpha_2^{-1}(0)$ just as we have proved before. This completes the proof. □

Remark 4. The stability of switching control of a boost converter is proved in [32]. The state space of the boost converter model is two dimensional, and the set $\alpha_1^{-1}(0) \cap \alpha_2^{-1}(0)$ is a singleton consisting of x^*. The state dimension of the zeta converter model is four, and the set $\alpha_1^{-1}(0) \cap \alpha_2^{-1}(0)$ includes the two-dimensional affine set spanned by d1 and d2 in (20). The stability of the operating point is a consequence of Theorem 1, which is a differential-inclusion version of LaSalle's invariance principle.

Remark 5. The switching mechanisms proposed in [29, 30, 31] basically pick up the mode which nearly decreases the Lyapunov function most while our method retains the mode as long as it decreases the Lyapunov function. The trajectory of [29] evolves as a sliding mode solution when it approaches the sliding boundary, which means that the switching interval becomes infinitesimally small. The sampled-data control approach in [30] and [31] can reduce the switching frequency by adjusting the sampling period. However, the period depends on the feasibility of matrix inequality, which is a sufficient condition and hence incurs conservativeness. Our method approaches a sliding mode solution only when the trajectory is near the operating point. Further reduction of switching frequency to the predetermined level is possible by using the modified switching mechanism stated in the next section.

4 | LIMITING THE SWITCHING FREQUENCY

The switching control proposed in Section 2 requires unbounded number of switching as a solution approaches the operating point x^*. In this section, the switching control mechanism discussed in Section 2 is modified to limit the switching frequency of a zeta converter.

4.1 | Modified switching mechanism

The switching mechanism considered in Section 2 is based on the signs of the derivatives along the trajectories (8) and (9). Let $\rho_1, \rho_2 > 0$ and $\tilde{\alpha}_1$ and $\tilde{\alpha}_2$ be modified switching functions which satisfy the following:

$$\tilde{\alpha}_1(x) \geq \alpha_1(x), \tilde{\alpha}_2(x) \geq \alpha_2(x), \tag{26}$$

$$\alpha_2^{(-1)}(\mathbb{R}_{(\geq 0)}) \subset \tilde{\alpha}_1^{(-1)}(\mathbb{R}_{(\leq \rho 1)}), \alpha_1^{(-1)}(\mathbb{R}_{(\geq 0)}) \subset \tilde{\alpha}_2^{(-1)}(\mathbb{R}_{(\leq \rho 2)}). \tag{27}$$

Notice that (27) is equivalent to

$$\tilde{\alpha}_1^{-1}\left(\mathbb{R}_{>\rho_1}\right) \subset \alpha_2^{-1}(\mathbb{R}_{<0}), \ \tilde{\alpha}_2^{-1}\left(\mathbb{R}_{>\rho_2}\right) \subset \alpha_1^{-1}(\mathbb{R}_{<0}).$$

Based on (26) and (27), we propose the following modified switching control mechanism:

Switching Mechanism B

- If the system is operating at mode 1 and reaches $\tilde{\alpha}_1^{-1}(\rho_1)$, then it switches to mode 2.
- If the system is operating at mode 2 and reaches $\tilde{\alpha}_2^{-1}(\rho_2)$, then it switches to mode 1.

The differential inclusion (12) is modified accordingly.

$$\frac{dx}{dt} \in \tilde{F}(x), \tag{28}$$

$$\tilde{F}(x) := \begin{cases} \{A_1 x + B_1 u_0\} & \text{if } x \in \tilde{M}_1, \\ \{A_2 x + B_2 u_0\} & \text{if } x \in \tilde{M}_2, \\ \text{conv}\{A_1 x + B_1 u_0, A_2 x + B_2 u_0\} & \text{if } x \in \tilde{M}_0, \end{cases}$$

where

$$\tilde{M}_1 = \left\{x : \alpha_1^{-1}(\mathbb{R}_{<0}) \cap \tilde{\alpha}_2^{-1}\left(\mathbb{R}_{>\rho_2}\right) = \tilde{\alpha}_2^{-1}\left(\mathbb{R}_{>\rho_2}\right)\right\},$$

$$\tilde{M}_2 = \left\{x : \tilde{\alpha}_1^{-1}\left(\mathbb{R}_{>\rho_1}\right) \cap \alpha_2^{-1}(\mathbb{R}_{<0}) = \tilde{\alpha}_1^{-1}\left(\mathbb{R}_{>\rho_1}\right)\right\},$$

$$\tilde{M}_0 = \left\{x : \tilde{\alpha}_1^{-1}\left(\mathbb{R}_{\leq\rho_1}\right) \cap \tilde{\alpha}_2^{-1}\left(\mathbb{R}_{\leq\rho_2}\right)\right\}.$$

Assumption 1. The sets $\tilde{\alpha}_1^{-1}(\mathbb{R}_{\leq\rho_1}) \cap \alpha_1^{-1}(\mathbb{R}_{>0})$ and $\tilde{\alpha}_2^{-1}(\mathbb{R}_{\leq\rho_2}) \cap \alpha_2^{-1}(\mathbb{R}_{>0})$ are bounded.

Proposition 6. *Suppose Assumption 1 holds. Let $c > 0$ satisfy*

$$c > \sup\left\{V(x) : x \in \left(\tilde{\alpha}_1^{-1}\left(\mathbb{R}_{\leq\rho_1}\right) \cap \alpha_1^{-1}(\mathbb{R}_{>0})\right) \cup \left(\tilde{\alpha}_2^{-1}\left(\mathbb{R}_{\leq\rho_2}\right) \cap \alpha_2^{-1}(\mathbb{R}_{>0})\right)\right\}.$$

Then for any solution $\tilde{\phi}(t, x_0)$ of (28), there exists $T > 0$ such that $\tilde{\phi}(t, x_0) \in \{x : V(x) < c\}$ for $t > T$.

Proof. First, we shall prove that $\tilde{F}(x) \subset F(x)$if $x \notin \Xi_\rho := (\tilde{\alpha}_1^{(-1)}(\mathbb{R}_{(\leq\rho 1)}) \cap \alpha_1^{(-1)}(\mathbb{R}_{(>0)}) \cup (\tilde{\alpha}_2^{(-1)}(\mathbb{R}_{(\leq\rho 2)}) \cap \alpha_2^{(-1)}(\mathbb{R}_{(>0)})$. From (27), $\tilde{\alpha}_1^{(-1)}(\mathbb{R}_{(>\rho_1)}) \subset \alpha_2^{(-1)}(\mathbb{R}_{(<0)})$. So, if $\tilde{\alpha}_2(x) > \rho_2$, then

$$\tilde{F}(x) = \begin{cases} \{A_1 x + B_1 u_0\} = F(x), \ \alpha_2(x) > 0, \\ \{A_2 x + B_2 u_0\} \subset conv\{A_1 x + B_1 u_0, A_2 x + B_2 u_0\} \\ \qquad = F(x), \ \alpha_2(x) \leq 0. \end{cases}$$

From Assumption 1, the number $c > 0$ exists. If $V(x_0) > c$, then a solution $\tilde{\phi}(t, x_0)$ of (28) satisfies $\tilde{\phi}(t, x_0) = \phi(t, x_0)$ as long as $\tilde{\phi}(t, x_0) \notin \Xi_\rho$ where $\phi(t, x_0)$ is a solution of (12). There exists $T > 0$ such that $V(\phi(t, x_0)) \geq c$ if $t > T$ because $V(\phi(t, x_0))$ is monotonically decreasing and $V(\phi(t, x_0)) \to 0$ as $t \to \infty$ from Theorem 1. Note that $\Xi_\rho \cap \{x : V(x) \geq c\} = \emptyset$. This implies that $\tilde{\phi}(t, x_0) = \phi(t, x_0)$ and $V(\tilde{\phi}(t, x_0)) \geq c$ for $0 \leq t \leq T$. Furthermore, $V(\tilde{\phi}(t, x_0))$ is non-increasing when $\tilde{\phi}(t, x_0) \notin \Xi_\rho$. Therefore, $V(\tilde{\phi}(t, x_0)) < c$ for $t > T$. □

4.2 | Example for the DC–DC zeta converter

From (19),

$$\alpha_1(x) = (x - x^*)^T \begin{bmatrix} 0 & 0 & 0 & 0 \\ 0 & 0 & 0 & 0 \\ 0 & 0 & 0 & 0 \\ 0 & 0 & 0 & -\frac{1}{R} \end{bmatrix} (x - x^*) + v_g\left(i_{L1} - i_{L1}^*\right) + v_g\left(i_{L2} - i_{L2}^*\right) - \frac{v_r}{R}\left(v_{C1} - v_{C1}^*\right), \tag{29}$$

$$\alpha_2(x) = (x - x^*)^T \begin{bmatrix} 0 & 0 & 0 & 0 \\ 0 & 0 & 0 & 0 \\ 0 & 0 & 0 & 0 \\ 0 & 0 & 0 & -\frac{1}{R} \end{bmatrix} (x - x^*) - v_r\left(i_{L1} - i_{L1}^*\right) - v_r\left(i_{L2} - i_{L2}^*\right) + \frac{v_r^2}{R}\left(v_{C1} - v_{C1}^*\right). \tag{30}$$

Define

$$d_3 := \begin{bmatrix} \frac{v_g R C_1}{L_1} \\ \frac{v_g R C_1}{L_2} \\ -v_r \\ 0 \end{bmatrix},\ d_4 := \begin{bmatrix} 0 \\ 0 \\ 0 \\ v_r \end{bmatrix}. \tag{31}$$

Then $\{d_1, d_2, d_3, d_4\}$ with d_1 and d_2 in (20) is a basis of $\mathbb{R}^4$, and thus any $x \in \mathbb{R}^4$ can be written as

$$x - x^* = \Delta x = \delta_1 d_1 + \delta_2 d_2 + \delta_3 d_3 + \delta_4 d_4. \tag{32}$$

The modified functions $\tilde{\alpha}_1(x)$ and $\tilde{\alpha}_2(x)$ can be defined as

$$\tilde{\alpha}_1(x) := \alpha_1(x) + k_1\delta_4^2 + \beta(c_1\delta_1, \delta_2), \tag{33}$$

$$\tilde{\alpha}_2(x) := \alpha_2(x) + k_2\delta_4^2 + \beta(c_2\delta_1, \delta_2), \tag{34}$$

where $\|\delta_1, \delta_2\|$ is any norm in $\mathbb{R}^2$, and $\beta : \mathbb{R}_{\geq 0} \to \mathbb{R}_{\geq 0}$ is a monotone non-decreasing function satisfying

$$\beta(0) = 0,\ \beta(z) = \rho,\ \text{if } z \geq \rho,$$

$$0 < k_1 \left\langle \frac{v_r^2}{R},\ 0 \left\langle k_2 \left\langle \frac{v_r^2}{R},\ c_1 \right\rangle 0,\ c_2 \right\rangle 0,\ \rho \right\rangle 0.$$

Proposition 7. *The functions $\tilde{\alpha}_1$ and $\tilde{\alpha}_2$ defined by (33) and (34) satisfy (26), (27), and Assumption 1.*

Proof. It is obvious that (26) holds. Suppose $\alpha_2(x) \geq 0$. Define $p_1(x - x^*) := \alpha_1(x) + k_1\delta_4^2$ and $p_2(x - x^*) := \alpha_2(x) + k_2\delta_4^2$. Then the quadratic terms of p_1 and p_2 are non-positive, and hence by Lemma 1, we assert that $\alpha_1(x) + k_1\delta_4^2 \leq 0$. Because $\beta(c_1\|\delta_1, \delta_2\|) \leq \rho_1$, we obtain $\tilde{\alpha}_1(x) \leq \rho_1$. Similarly, $\alpha_1(x) \geq 0$ implies $\tilde{\alpha}_2(x) \leq \rho_2$. To show that $\alpha_1^{-1}(\mathbb{R}_{>0}) \cap \tilde{\alpha}_1^{-1}(\mathbb{R}_{\leq\rho 1})$ is bounded, we use the representation (30) and show that the set $\{(d_1, d_2, d_3, d_4) : x \in \alpha_1^{(-1)}(\mathbb{R}_{(>0)}) \cap \tilde{\alpha}_1^{(-1)}(\mathbb{R}_{(\leq\rho 1)})\}$ is bounded. If $\alpha_1(x) > 0$ and $\tilde{\alpha}_1(x) \leq \rho_1$, then

$$\rho_1 > \tilde{\alpha}_1(x) - \alpha_1(x) = k_1\delta_4^2 + \beta(c_1\delta_1, \delta_2) \geq \begin{cases} \beta(c_1\delta_1, \delta_2), \\ k_1\delta_4^2. \end{cases} \tag{35}$$

From (35), it follows that $\|\delta_1, \delta_2\| < \frac{\rho_1}{c_1}$ and $|\delta_4| < \sqrt{\frac{\rho_1}{k_1}}$. From the definition of α_1, $\tilde{\alpha}_1$, and d_3, we have

$$\alpha_1(x) = k\delta_3 + \gamma(\delta_1, \delta_2, \delta_4), \quad \tilde{\alpha}_1(x) = k\delta_3 + \tilde{\gamma}(\delta_1, \delta_2, \delta_4),$$

where γ and $\tilde{\gamma}$ are continuous functions and

$$k = \frac{v_r^2 R C_1}{L_1} + \frac{v_r^2 R C_1}{L_2} + \frac{v_r^2}{R} > 0.$$

Let

$$M := \sup\left\{\gamma(\delta_1, \delta_2, \delta_4) :\ \delta_1, \delta_2 < \frac{\rho_1}{c_1}, |\delta_4| < \sqrt{\frac{\rho_1}{k_1}}\right\},$$

$$m := \inf\left\{\tilde{\gamma}(\delta_1, \delta_2, \delta_4) :\ \delta_1, \delta_2 < \frac{\rho_1}{c_1}, |\delta_4| < \sqrt{\frac{\rho_1}{k_1}}\right\}.$$

Then,

$$0 < \alpha_1(x) = k\delta_3 + \gamma(\delta_1, \delta_2, \delta_4) \leq k\delta_3 + M,$$

$$\rho_1 \geq \tilde{\alpha}_1(x) = k\delta_3 + \tilde{\gamma}(\delta_1, \delta_2, \delta_4) \geq k\delta_3 + m,$$

and it follows that $-\frac{M}{k} < \delta_3 \leq \frac{\rho_1 - m}{k}$. The boundedness of the set $\alpha_2^{-1}(\mathbb{R}_{>0}) \cap \tilde{\alpha}_2^{-1}(\mathbb{R}_{\leq\rho 2})$ can be proved similarly. □

Remark 6. From Proposition 6 and 7, we conclude that any solution of (28) converges to the set $\{x : V(x) < c\}$. The spatial regularization was studied for the boost converter in [29] to reduce the high rate of switching. The method discussed in this section extends the idea to the zeta converter by adding extra terms in (33) and (34) to cope with the four-dimensional state space.

4.3 | Estimating the switching frequency

Although the modified switching mechanism is able to limit the switching frequency, the value of the switching frequency itself, however, is controlled by the parameters in Switching Mechanism B. In this subsection, we will show how to decide such parameters based on a linear-line approximation of the trajectory.

From Section 4.2, the switching occurs when

$$\rho_1 := \tilde{\alpha}_1(x^* + \Delta x_1),$$

$$\rho_2 := \tilde{\alpha}_2(x^* + \Delta x_2),$$

where $\Delta x_1 := [\Delta i_{L1a} \Delta i_{L2a}\ \ \Delta v_{C1a}\ \ 0]^T$ and $\Delta x_2 := [\Delta i_{L1b}\ \Delta i_{L2b}\ \Delta v_{C1b}\ 0]^T$ are the difference of the approximated state-trajectory from the operating point at their respective switching instants as shown in Figure 4.

Observing Figure 4 and from (21) and (22), the gradient of the state-trajectory at the operating point is given by

$$\frac{2\Delta x_1}{\lambda T_{sw}} = \begin{bmatrix} \frac{v_g}{L_1} \\ \frac{v_g}{L_2} \\ -\frac{v_r}{C_1 R} \\ 0 \end{bmatrix},\quad \frac{2\Delta x_2}{(1-\lambda) T_{sw}} = \begin{bmatrix} -\frac{v_r}{L_1} \\ -\frac{v_r}{L_2} \\ \frac{v_r^2}{C_1 R v_g} \\ 0 \end{bmatrix},$$

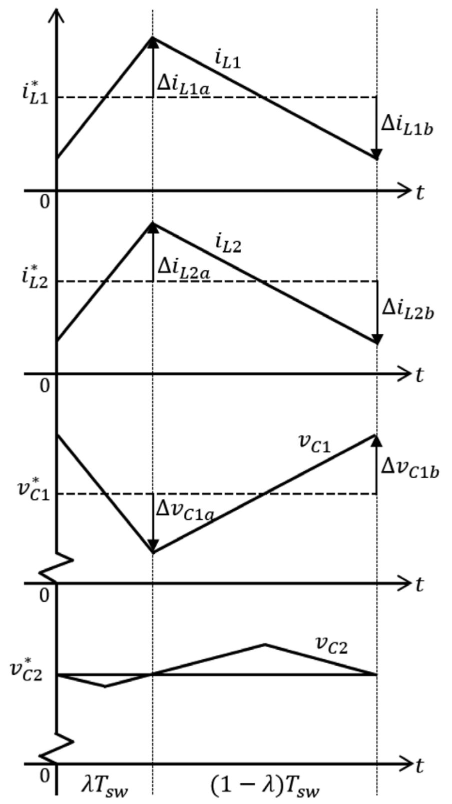

FIGURE 4 Approximate state-trajectory

where $T_{sw} = \frac{1}{f}$ is the period of the switching frequency f. With $\lambda = \frac{v_r}{v_r+v_g}$ (from (17)) the above expressions can be rewritten as

$$\Delta x_1 = \begin{bmatrix} \frac{v_r v_g}{2fL_1(v_r+v_g)} \\ \frac{v_r v_g}{2fL_2(v_r+v_g)} \\ -\frac{v_r^2}{2fC_1R(v_r+v_g)} \\ 0 \end{bmatrix}, \quad \Delta x_2 = \begin{bmatrix} -\frac{v_r v_g}{2fL_1(v_r+v_g)} \\ -\frac{v_r v_g}{2fL_2(v_r+v_g)} \\ \frac{v_r^2}{2fC_1R(v_r+v_g)} \\ 0 \end{bmatrix}. \tag{36}$$

Define penalty functions $\sigma_1 := k_1\delta_4^2 + \beta(c_1\delta_1, \delta_2)$ and $\sigma_2 := k_2\delta_4^2 + \beta(c_2\delta_1, \delta_2)$ and assume the state-trajectory near the operating point. Therefore, the penalty functions are close to 0 such that $\sigma_1 \approx 0$ and $\sigma_2 \approx 0$, consequently, $\rho_1 \approx \alpha_1(x^* + \Delta x_1)$ and $\rho_2 \approx \alpha_2(x^* + \Delta x_2)$. Nevertheless, the effect of $\sigma_1 > 0$ and $\sigma_2 > 0$ will be investigated and illustrated graphically later in Section 5. Therefore, with (17) and (36), and from (29) and (30), we have

$$\rho_1 \approx \frac{v_r\left(L_1L_2v_r^2 + C_1L_1R^2v_g^2 + C_1L_2R^2v_g^2\right)}{2fC_1L_1L_2R^2\left(v_r+v_g\right)}, \tag{37}$$

$$\rho_2 \approx \frac{v_r^2\left(L_1L_2v_r^2 + C_1L_1R^2v_g^2 + C_1L_2R^2v_g^2\right)}{2fC_1L_1L_2R^2v_g\left(v_r+v_g\right)}. \tag{38}$$

TABLE 1 The DC–DC zeta converter parameters

Parameter	Value
v_g	18 V
$v_o(v_{ref})$	5 V
R	2.5 Ω
L_1	100 μH
L_2	100 μH
C_1	100 μF
C_2	220 μF
f	100 kHz

From (37) and (38), we observe how the desired switching frequency f is related to the thresholds ρ_1 and ρ_2. Therefore, the DC–DC zeta converter will operate at the prescribed switching frequency under the modified switching rule. Though the expressions of ρ_1 and ρ_2 look complex, they are straightforwardly processed beforehand (offline). Nowadays, considering the capability of the high-speed processors like in the DSP, FPGA, or even (maybe) microcontroller, there should be no performance issue in executing the switching mechanism.

5 | SIMULATION RESULTS

The simulations are carried out using the circuit simulation software PSIM® with the parameters shown in Table 1. With the input voltage v_g, the capacitor voltage v_{C2}, and the load current i_o are the variables that are sensed in the circuit in Figure 1, and fixed number computation instead of floating-point computation is used practically to reduce computational burden; ρ_1 and ρ_2 in (37) and (38), respectively, can be rewritten as

$$\rho_1 \approx \frac{25}{100\left(v_g+5\right)}\left(25\left(\frac{i_o}{v_{C2}}\right)^2 + \left(v_g^2+1\right)\right),$$

$$\rho_2 \approx \frac{125}{100v_g\left(v_g+5\right)}\left(25\left(\frac{i_o}{v_{C2}}\right)^2 + \left(v_g^2+1\right)\right).$$

In Figure 5, the simulation results for $\sigma_1 \approx 0$ and $\sigma_2 \approx 0$ are shown. As can be seen, with the nominal $v_g = 18$ V and $i_o = 2$ A, no overshoot for the output voltage v_o is observed at the start-up, and the settling time is approximately 10 ms. At $t = 20$ ms, v_g drops to 9 V and i_o reduces to 1 A. Despite the large input voltage drops, the overshoot at the output voltage is considerably small with some oscillations can be seen before it settles down at approximately $t = 30$ ms. Afterwards, at $t = 40$ ms, the input voltage drops further to 3 V and $i_o = 0.33$ A. Similarly, although more oscillation and longer setting time are observed, nonetheless the output voltage is able to return to its operating point. Moreover, the converter is now operating in step-up mode (instead of step-down mode for the first two perturbations), thus proving the effectiveness of the switching

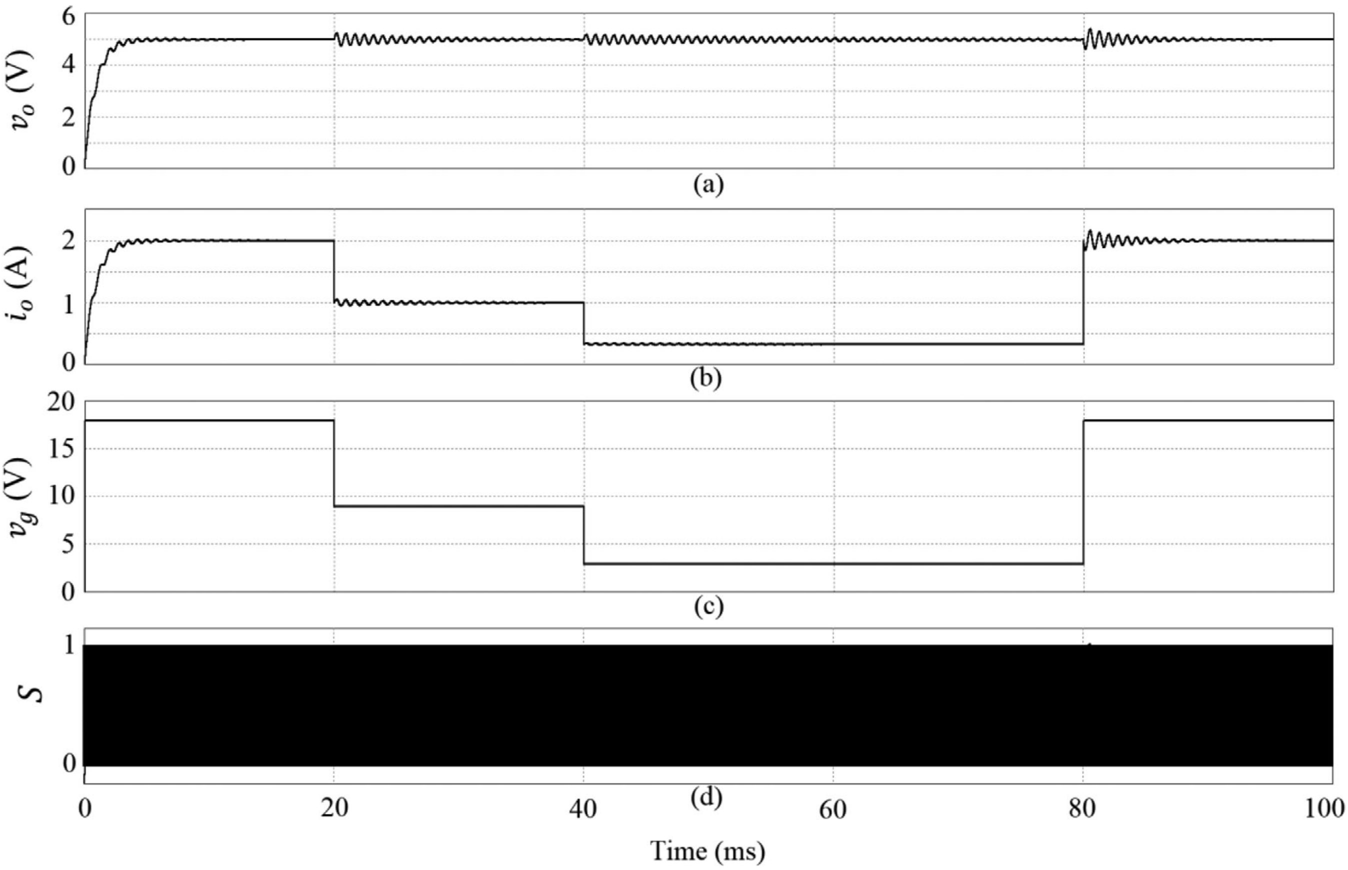

FIGURE 5 Simulation results under perturbations with $\sigma_1 \approx 0$ and $\sigma_2 \approx 0$. Variations in (a) the output voltage v_o, (b) the output current i_o, (c) the input voltage v_g, and (d) the switching waveform S

control in regulating the output voltage at both operation modes. Finally, at $t = 80$ ms, the input voltage returns to its nominal value of 18 V. Although the increment is very significant (+500%), the switching control can regulate the output voltage well with minimum overshoot (approximately 10%) and considerably fast settling time (approximately 8 ms). On the other hand, the steady-state switching waveforms in close view for the three different input voltage perturbations are illustrated in Figure 6. As shown, the switching control algorithm is able to produce the desired switching frequency of appoximately 100 kHz for all three instances.

In the next simulation, the effect of introducing the penalty functions $\sigma_1 > 0$ and $\sigma_2 > 0$, defined in Section 4, are shown in Figure 7. As can be observed, the introduction of σ_1 and σ_2 does not have much effect on the response of the output voltage. Increasing σ_1 and σ_2, hovewer, increases the switching frequency as shown in Figure 8. These observations are expected: (37) and (38) are no longer valid, since σ_1 and σ_2 are not approximately zero. As σ_1 and σ_2 reache ρ_1 and ρ_2, respectively, the number of switching becomes unbounded, which is identical for the case of the switching control mechanism in Section 2.

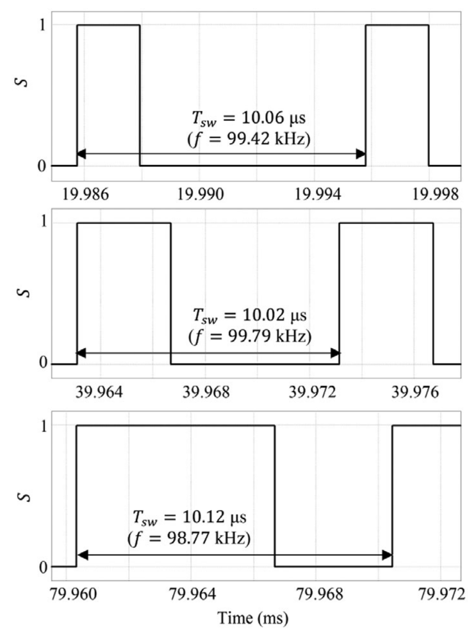

FIGURE 6 Close view of the switching waveform S when $v_g = 18\ V$ (top), $v_g = 9\ V$ (middle), and $v_g = 3\ V$ (bottom)

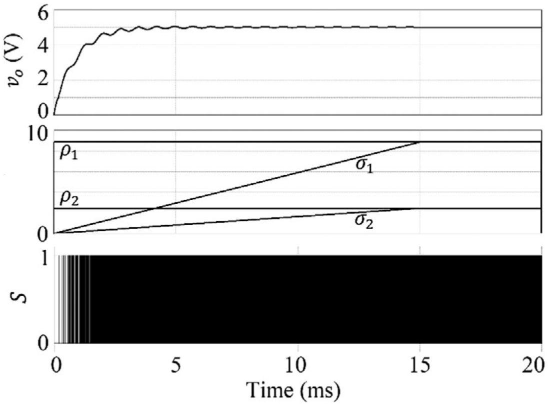

FIGURE 7 Simulation results for $\sigma_1 > 0$ and $\sigma_2 > 0$

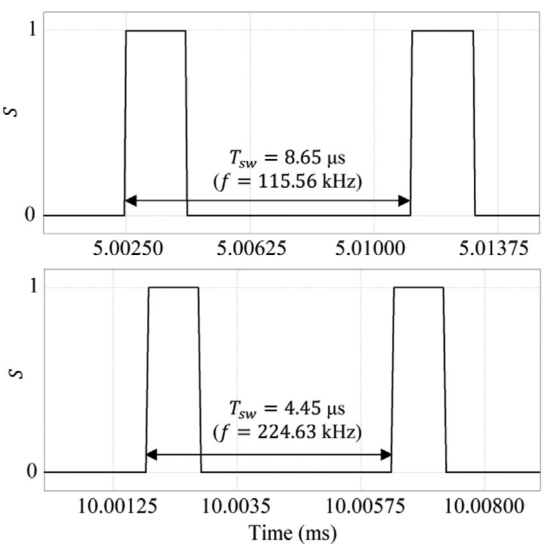

FIGURE 8 Close view of the switching waveform S corresponds to $\sigma_1 = 2.95, \sigma_2 = 0.82$ (top) and $\sigma_1 = 5.90, \sigma_2 = 1.64$ (bottom)

6 | CONCLUSION AND FUTURE WORK

Here, we have presented a switching control mechanism which induces closed-loop stability of the DC–DC zeta converter. A two-mode system is use to model the DC–DC zeta converter operating in CCM. A switching control algorithm is derived from a Lyapunov functional candidate which is basically the energy storage function of the zeta converter. Instrumental in our work is the establishment of an analysis of the fourth-order zeta converter that is simple but sufficient to prove the stability of the control. Moreover, our switching control mechanism is not only able to reduce the switching frequency, but most essentially one can systematically choose the desired switching frequency for the converter to operate. Important to highlight here is how we use two different thresholds ρ_1 and ρ_2 (for mode 1 and mode 2, respectively) to define the spatial regularization, as opposed to a single common threshold for the two modes as adapted in [32]. As a result, we were able to solve the switching control flaw in [32] by eliminating the output voltage steady-state error. Although the approximate state waveforms are used to find ρ_1 and ρ_2, the close agreement between the theoretical and simulation results of the desired switching frequency shows that the approximation is indeed justified. In future, we plan to add the internal resistances in the zeta converter model, consider the effect of interference, and most importantly validate the findings with experimental results.

ACKNOWLEDGEMENTS

The first author would like to thank Universiti Teknikal Malaysia Melaka and the Ministry of Higher Education Malaysia for the financial support. The work of the second and the third authors was supported by JST CREST Grant Number JPMJCR15K1, Japan.

ORCID

Hafez Sarkawi https://orcid.org/0000-0003-3117-2801

REFERENCES

1. Sarkawi, H., Ohta, Y., Rapisarda, P.: Preliminary finding on the switching control algorithm for the stabilization of the DC-DC zeta converter. In: Proceedings of SICE Annual Conference, Nara, Japan, pp. 971–974 (2018)
2. Sarkawi, H., Ohta, Y., Rapisarda, P.: Comparative study of PWM-based versus hybrid control for the DC-DC zeta converter voltage regulation. In: Proceedings of SICE International Symposium on Control Systems, Kumamoto, Japan, pp. 498–504 (2019)
3. Bayat, F., Karimi, M., Taheri, A.: Robust output regulation of zeta converter with load/input variations: LMI approach. Contr. Eng. Practice. 84(3), 102–111 (2019)
4. Peres, A., Martins, D.C., Barbi, I.: ZETA converter applied in power factor correction. In: Proceedings of IEEE Conference on Power Electronics Specialist, Taipei, Taiwan, pp. 1152–1157 (1994)
5. Ramirez, J.A., et al.: A stable design of PI control for DC-DC converters with an RHS zero. IEEE Trans. Ind. Appl. 48(1), 103–106 (2001)
6. Vuthchhay, E., Bunlaksananusorn, C.: Modeling and control of a zeta converter. In: Proceedings of IEEE International Power Electronics Conference, Sapporo, Japan, pp. 612–619 (2010)
7. Chen, Z.: PI and sliding mode control of a CUK converter. IEEE Trans. Pow. Electron. 27(8), 3695–3703 (2012)
8. Garg, M.M., Hote, Y.V., Pathak, M.K.: PI controller design of a dc-dc zeta converter for specific phase margin and cross-over frequency. In Proceedings of IEEE Asian Control Conference, Sabah, Malaysia, pp. 1–6 (2015)
9. Sarkawi, H., Ohta, Y.: Optimal state-feedback and proportional-integral controller performance comparison for DC-DC zeta converter operating in continuous conduction mode. In: Proceedings of SICE Annual Conference, Tsukuba, Japan, pp. 448–451 (2016)
10. Rodriguez, E., et al.: General-purpose ripple-based fast-scale instability prediction in switching power regulators. In: Proceedings of IEEE ISCAS, New Orleans, pp. 2423–2426 (2007)
11. Sarkawi, H., et al.: Dynamic model of zeta converter with full-state feedback controller implementation. Int. Jour. Research Eng. Tech. 2(8), 34–43 (2013)
12. Olala, C., et al.: Robust LQR control for PWM converters: An LMI approach. IEEE Trans. Ind. Electron. 56(7), 2548–2558 (2009)
13. Olala, C., et al.: Optimal state-feedback control of bilinear DC-DC converters with guaranteed regions of stability. IEEE Trans. Ind. Electron. 59(10), 3868–3880 (2012)
14. Sarkawi, H., Ohta, Y.: Comparison of conventional LQR and LMI based LQR controller performance on the DC-DC zeta converter with parameters uncertainty. In: Proceedings of Multi-symposium on Control Systems, Okayama, Japan, pp. 642–647 (2017)
15. Sarkawi, H., Ohta, Y.: Uncertain DC-DC zeta converter control in convex polytope model based on LMI approach. Int. Jour. Pow. Electron. Drive Sys. 9(2), 829–838 (2018)

16. Olala, C., Leyva, R., Queinnec, I.: Robust gain-scheduled control of switched-mode DC–DC converters. IEEE Trans. Pow. Electron. 27(6), 3006–3019 (2012)
17. Wang, C., et al.: Discretisation performance analysis of sliding mode controlled DC–DC buck converter via zero-order holder. IET Cont. Theory Appl. 13(16), 2583–2594 (2019)
18. Tan, S.-C., et al.: A fast response sliding mode controller for boost-type converters with a wide range of operating conditions. IEEE Trans. Ind. Electron. 54(6), 3276–3286 (2007)
19. Lam, H.K., Tan, S.C.: Stability analysis of fuzzy-model-based control systems: Application on regulation of switching DC–DC converter. IET Cont. Theory Appl. 3(8), 1093–1106 (2009)
20. Khateb, A.E., et al.: Fuzzy-logic-controller-based SEPIC converter for maximum power point tracking. IEEE Trans. Ind. Appl. 50(4), 2349–2358 (2014)
21. Cavanini, L., et al.: Model predictive control for pre-compensated voltage mode controlled DC–DC converters. IET Cont. Theory Appl. 11(15), 2514–2520 (2017)
22. Kim, S-K., et al.: Output-feedback model predictive controller for voltage regulation of a DC/DC converter. IET Cont. Theory Appl. 7(16), 1959–1968 (2013)
23. Cheng, Y., et al.: Fast adaptive finite-time voltage regulation control algorithm for a buck converter system. IEEE Trans. Cir. Sys. II: Express Briefs 64(9), 1082–1086 (2014)
24. Wai, R.J., Shih, L.C.: Adaptive fuzzy-neural-network design for voltage tracking control of a DC–DC boost converter. IEEE Trans. Pow. Electron. 27(4), 2104–2115 (2012)
25. Sreekumar, C., Agarwal, V.: Hybrid control approach for the output voltage regulation in buck type DC–DC converter. IET Elec. Pow. Appl. 1(6), 897–906 (2007)
26. Sreekumar, C., Agarwal, V.: A hybrid control algorithm for voltage regulation in DC–DC boost converter. IEEE Trans. Ind. Electron. 55(6), 2530–2538 (2008)
27. Sreekumar, C., Agarwal, V.: Hybrid control of boost converter operating in discontinuous current mode. In: IEEE Conference on Power Electronics Specialists, Jeju, South Korea, pp. 255–260 (2006)
28. Hongbo, M., Quanyuan, F.: Hybrid modeling and control for buck-boost switching converters. In: Proceedings of IEEE International Conference on Commication, Circuits and Systems, California, pp. 678–682 (2009)
29. Deaecto, G., et al.: Switched affine systems control design with application to dc-dc converters. IET Cont. Theory Appl. 4(7), 1201–1210 (2010)
30. Hetel, L., Fridman, E.: Robust sampled-data control of switched affine systems. IEEE Trans. Auto. Cont. 58(11), 2922–2928 (2013)
31. Yan, X., et al.: Sampled-data control with adjustable switching frequency for dc-dc converters. IEEE Trans. on Ind. Electron. 66(10), 8060–8071 (2019)
32. Theunisse, T.A.F., et al.: Robust global stabilization of the DC-DC boost converter via hybrid control. IEEE Trans. Cir. Sys.–I: Reg. Papers 62(4), 1052–1061 (2015)
33. Vidyasagar, M.: Nonlinear systems analysis (2nd edn.). Prentice-Hall (1993)
34. Aubin, J.-P., Cellina, A.: Differential inclusions (1st edn.). Springer-Verlag (1984)

How to cite this article: Sarkawi H, Ohta Y, Rapisarda P. On the switching control of the DC–DC zeta converter operating in continuous conduction mode. *IET Control Theory Appl.* 2021;15:1185–1198. https://doi.org/10.1049/cth2.12115